SCRIPPS INSTITUTION OF OCEANOGRAPHY

9500 GILMAN DRIVE
LA JOLLA, CA 92093-0208

Brian Robertson, Chief   February 21, 2020
Off Highway Motor Vehicle Recreation Division
California Department of Parks and Recreation
1725 23rd Street, Suite 200
Sacramento CA 95816

Dear Chief Robertson,

    Please find attached our report of findings regarding aerosolized particulates in south San Luis Obispo County. As stated in the report, we found that during high prevailing wind conditions natural sea salt and inert mineral dust measured in the PM2.5 fraction at the CDF location together account for only 30% to 50% of the PM2.5 measured at the same location by BAM instrumentation operated by the local air district (SLOAPCD).

    There was only a small contribution of fossil fuel combustion emissions to PM2.5 at the CDF location which indicates that PM2.5 is not a good predictor of toxic emissions or health effects in high wind conditions.

    Our results suggest the high dust concentrations measured on high wind days in and downwind of Oceano Dunes are likely dominated by natural saltation processes associated with the indigenous geomorphological dune structure.

    We also found that there is a significant discrepancy in PM2.5 mass when comparing mass as measured by the SLOAPCD CDF PM2.5 BAM with the chemical mass of PM2.5 samples collected at the CDF location for this investigation. For this reason, offline chemical and gravimetric analyses would be needed in order to determine whether the SLOAPCD CDF BAM data are representative of actual PM2.5 concentrations at the CDF location and to determine what fraction of PM2.5 is dust.

    We would like to extend our appreciation to the California Geological Survey and to the California Department of Parks and Recreation for the assistance and access that made our investigation possible. We look forward to continued collaboration as this project continues.

    Sincerely on behalf of all investigators,

Brian Palenik
Professor of Marine Biology SIO
UC San Diego
La Jolla, CA 92093
bpalenik@ucsd.edu
858-534-7505

First Year (2019) Summary Report:
Investigation of Aerosol Particulates in a Coastal Setting, South San Luis Obispo County, California.

By:
Lynn Russell
Mati Kahru
Brian Palenik

Scripps Institution of Oceanography
University of California San Diego
La Jolla, CA 92093-0202
Contact information: bpalenik@ucsd.edu

Submitted 2/21/2020

Introduction

Building upon the results of the 6 March 2018 report by Palenik, this project has undertaken additional deoxyribonucleic acid (DNA) sampling of various environmental media and new quantitative chemical sampling to improve the understanding of the sources of airborne particle mass (or particulate matter, PM) in a region of south San Luis Obispo (SLO) County, California. Specifically, the region includes extensive coastal sand dunes found south of Pismo Beach, California, as well as an upland area approximately 3.2 kilometers (km) (two miles) east of the coastline known as Nipomo Mesa. A California state park called Oceano Dunes lies within the coastal dunes. On approximately 1,000 acres within the park and larger dune area, the California Department of Parks and Recreation provides opportunity for vehicle access to the coast, camping, and off-highway vehicle (OHV) recreation. The dune system is fueled by an ample supply of offshore sediment and strong prevailing winds from the west-northwest which occur seasonally in the spring and fall. The Nipomo Mesa area is downwind of this dune system.

The project primarily included collecting PM samples on Teflon air filters at a location within the OHV riding area of Oceano Dunes and from the Nipomo Mesa area. The dune location for sampling is called S1 and was chosen because it is co-located with a meteorological station and is relatively close to the shoreline (approximately 410 meters, or about 1,350 feet), with relatively minimal OHV recreation occurring between S1 and the shoreline. The Nipomo Mesa sample location is called CDF because it is at a California Department of Forestry and Fire Protection fire station along California State Highway 1, and approximately 3.7 km (2.3 miles) downwind (south-southeast) of the S1 site. This site was chosen because of its downwind location and because it is the same location where the San Luis Obispo County Air Pollution Control District (SLOAPCD) operates an air quality monitoring station, which is also called CDF.

In 2019, this project included two sampling periods, one in May and the other in late September and early October. The objectives of the research were to:

1) Quantify the organic and elemental components of PM2.5 aerosol particles (PM that is 2.5 microns or less in diameter) collected at the CDF site;
2) Show the contribution of PM1 (PM that is one micron or less in diameter) to PM2.5 particle mass at CDF;
3) Compare the mass of PM2.5 samples collected at the CDF site with those collected at the near-shoreline dune location, S1;
4) Extend sampling of DNA from seawater, beach foam, and aerosol particles to test efficacy of Teflon air filters.
5) Characterize photosynthetic activity of phytoplankton offshore from the south San Luis Obispo County region.

The PM concentration in the south SLO County region is expected to be contributed by a mixture of organic and inorganic components from natural and man-made sources. The seaside location means that sea spray from breaking waves and whitecaps in the ocean will contribute particles with salt (NaCl as well as some trace additional salts) and organic components (from nutrients and exudates that are produced and consumed by marine biota such as phytoplankton) [Russell et al., 2010]. Another proximate natural source is mineral dust from the sand dunes. Both sea spray and sand dust increase with increasing wind speed as well as with the surface area covered (by ocean or sand, respectively) and proximity to that area (of ocean or sand, respectively). Both sea spray and dust have substantial supermicron PM contributions (namely particles larger than 1 micron diameter) that have short atmospheric lifetimes. Neither sea spray nor blown mineral dust from sand dunes has been associated with evidence of chronic respiratory effects since (1) most supermicron inhaled components are removed by impaction in the nasal passages and upper airways and (2) sea spray and inert mineral dust are not composed of toxic compounds.

In addition to these natural sources, local emissions associated with motor vehicles [Russell et al., 2011], residential and commercial activities (including use of personal care products) [McDonald et al., 2018], food preparation and heating [Chen et al., 2018], seasonal agricultural harvesting and fertilizing, wildfires, and long-range transport from high-population areas (from Asia as well as closer urban areas) also contribute both organic and inorganic particle mass to PM2.5 and PM10 (PM that is 10 microns or less in diameter), with the contribution from each varying with wind direction as well as other conditions.

PM2.5 and PM10 are regulated by U.S. and California clean air standards because of their known association with degraded visibility and detrimental health effects [US Clean Air Act (https://www.epa.gov/laws-regulations/summary-clean-air-act); Dockery et al., 1993; Pope et al., 2009; Apte et al., 2018]. Recently, Apte et al. calculated the U.S. average life expectancy decrement to be 0.38 yr for PM2.5, which is three times lower than that of countries with higher PM2.5 (e.g. China, India). While the availability of PM2.5 measurements makes it the best proxy for epidemiological studies of populations, physiological studies of health effects

have shown that the causes of cell degradation from PM2.5 inhalation are most likely from specific toxic compounds, such as polycyclic aromatic hydrocarbons that are associated with fossil fuel combustion and black carbon. Recent evidence also suggests that nanoparticles (particles that are less than 0.1 micron in diameter) and transition metals, both of which are also associated with fossil fuel combustion, may play important detrimental and causative roles as well [Knol et al., 2009; Oberdorster et al., 2007; Gwinn and Vallyathan, 2006; Janssen et al., 2003; Hoek et al., 2002]. Since the association of PM2.5 with toxics and nanoparticles is likely responsible for the association of PM2.5 with health effects, the use of PM2.5 as a health indicator may fail when PM2.5 is not co-emitted with those toxics and nanoparticles.

It is worth noting that there is no evidence that toxic compounds are associated with elevated PM concentrations detected downwind of the south SLO County sand dunes during windy conditions. The two major sources of PM in this area (mineral dust from dune processes and sea spray) are larger than 0.1 micron and are from non-toxic natural sources so association of PM2.5 with detrimental health effects may be without foundation. Urban locations serve as the basis for epidemiological health studies because of large population density [Dockery et al. 1993; Pope et al. 2009], and PM2.5 in these locations is largely associated with emissions from motor vehicles which include high amounts of toxics, nanoparticles, and transition metals [Q. Zhang et al. 2007; J. Jimenez et al. 2009; NARSTO 2004]. To date, there is no evidence that in areas where PM2.5 is dominated by natural emission sources rather than by man-made combustion emissions that the causal link between PM2.5 and health effects would hold. For this reason, assessing whether health effects are associated with PM2.5 requires identifying what fraction of PM2.5 is from natural (non-toxic) sources and what fraction is from combustion emissions.

The chemical composition of PM2.5 provides the first critical step for identifying how much of particle mass is associated with each of these different sources. Here we use Fourier Transform Infrared (FTIR) and X-ray Fluorescence (XRF) spectroscopy to provide a first cut at these sources, using elemental composition to provide tracers for sea spray, mineral dust, and combustion emissions, and organic composition to distinguish between biological organics (marine and terrestrial with high alcohol to alkane ratios) and combustion organics (fossil fuel or biomass-burning related).

Results

In 2019, samples were collected for 20 days at the CDF location for the period of 14 May 2019 to 2 June 2019 (hereafter "May 2019") and an additional 12 days of sampling from 23 September 2019 to 5 October 2019 (hereafter "October 2019"). The CDF site was co-located with the CDF air monitoring station operated by the SLOAPCD. The SLOAPCD CDF site includes hourly monitoring of PM2.5 and PM10 using continuous beta attenuation monitors (BAMs). The SLOAPCD BAM measurements provide a metric representing the PM2.5 (or PM10) concentration at ambient conditions, where that mass is measured when including water and semi-volatile organic and inorganic components (notably ammonium nitrate). The number of sampling days was maximized to document the day-to-day variability in the aerosol and to capture multiple days with high PM2.5 concentration.

The S1 site was sampled for 12 days from 23 September 2019 to 5 October 2019, with some periods lost due to power outages. The S1 site was selected to provide a benchmark for ocean and dunes sources, since it is located within the dunes and within a short distance of the shoreline, as indicated previously.

During the period of 14 May 2019 to 2 June 2019 there were 10 days when hourly PM10 as measured by SLOAPCD BAM exceeded 40 micrograms per cubic meter ($\mu g\ m^{-3}$), but only one of those days was on a weekend (25 May 2019) and one on a holiday (27 May 2019), so that eight days were week days when OHV traffic in the park is typically lower. Climatological data were used to schedule sampling during high-wind seasons (notably May and October). Short-term forecasts of high-wind conditions were usually predictive of high PM days.

The results addressing the objectives of the research are summarized below:

1. Quantify the organic and elemental components of PM2.5 aerosol particles collected at the CDF site: The organic and elemental components of PM2.5 aerosol particles were measured at CDF in May and October of 2019.

    a. The organic components identified in the samples indicate a variety of particle sources during different time periods. Figures 1, 2, and 3 show the organic functional group (OFG) measurements by FTIR for samples that had quantities significantly above detection limit. Note that a high alkane OFG mass is likely representative of fossil fuel combustion emissions from man-made sources, and that a high ratio of alcohol OFG mass to alkane OFG mass is indicative of marine sea spray organic sources (e.g., phytoplankton). The May and October FTIR measurements show qualitatively that there were different sources of organic mass present since the mixture of OFG varies from day to day. The two types of mixtures evident in the FTIR analyses of the samples collected: One shows a high ratio of alcohol OFG mass to alkane OFG mass, indicating sea spray. The other mixture is mostly alkane OFG mass with amine OFG mass, which may indicate either fossil fuel combustion (including vehicles) or sea spray. Some samples are a mixture of both of these two types. There are also carboxylic acid groups present in a majority of samples, which typically indicate oxidation of volatile organic carbon emissions by photochemistry.

    b. Using two methods, the elemental components of a limited number of samples were determined to estimate the mass of mineral dust. The first method is a standard approach based on the most common oxides for the non-sea-salt (nss) elements measured and is named "nss dust" [Usher et al., 2003], while the second approach used aerosolized and size-separated PM generated in the laboratory from a bulk sample of surface dune sand collected adjacent to the S1 site. The collected dune sand was not dried prior to being aerosolized in the laboratory and so some water was retained. Salts that are present in sand (including NaCl, ammonium nitrate, and ammonium sulfate) will take up water once the relative humidity (RH) is high enough to exceed the solubility limit (deliquescence point) of the salt [Seinfeld and Panids, 2006]. The result is that when salts are in contact with humid air, some liquid water forms on the salts

and becomes associated with the sand until it is dried out. Accordingly, this second method is named "wet dust." These two approaches provide estimates for the mineral component mass (nss dust) and for the higher mass that could be associated with dust at ambient relative humidity (wet dust). The comparison of the two approaches shown in Figure 4 indicates that the "wet dust" approach accounted for approximately 50% additional mass from water. This means that the two methods are consistent in terms of the amount of mass associated with specific measured elements. It also provides preliminary evidence that water could be a substantial fraction (50%) of both surface sand and lofted dust.

c. The measured PM2.5 components for May and October are shown in Figures 5 and 6. For May samples for which SLOAPCD BAM measurements of PM2.5 exceeded 20 µg m-3 and all chemical components were above detection (May 17, 22, and 28), the sea salt, nss dust, organic compounds, and sulfate accounted for 38% to 57% of the averaged hourly BAM PM2.5 measurements, indicating a PM2.5 mass discrepancy between samples collected for this investigation and temporally corresponding PM2.5 mass measurements made by the SLOAPCD CDF BAM. For days in May 2019 with BAM 2.5 exceeding 20 µg m^{-3}, sea salt varied from 1.1 to 1.8 µg m^{-3}, corresponding to 4% to 7% of BAM PM2.5, and nss dust from 4.1 to 14.4 µg m^{-3}, corresponding to 26% to 46% of BAM PM2.5. Organic components contributed only 1.1 to 1.8 µg m^{-3}, which was less than 6% of BAM PM2.5 on days with BAM PM2.5 exceeding 20 µg m^{-3}.The remaining 43% to 62% of mass indicated by the CDF BAM measurements could be water or ammonium nitrate, as these components were not measured but are commonly found in PM2.5 [Seinfeld and Pandis, 2006].

d. PM2.5 mass concentrations of fossil-fuel related components (alkane groups and transition metals) were well below 5 µg m-3, with most combustion-related metals at trace levels only, as is expected for a coastal location with relatively low population density.

2. <u>Show the contribution of PM1 to PM2.5 particle mass at CDF</u>: The May 2019 results show that PM1 and PM2.5 are often closely related. The organic mass concentration for the May 2019 CDF samples range from 0.5 to 2.5 µg m^{-3} of PM2.5, with a lower range on average for PM1. For the nine samples that overlapped in timing, the PM1 organic mass concentration average was 0.38 µg m^{-3} and PM2.5 average was 0.78 µg m^{-3}. These averages indicate that about half of the PM2.5 organic mass was in particles smaller than PM1, and the remaining half was between the sizes of 1 and 2.5 micron ambient diameter. Larger ratios than one half are typical for measurements made at dry diameters [Takahama et al., 2011], but the high seaside relative humidity (RH) means that PM1 captures a smaller fraction of particles. This happens because salts that are present in particles (including NaCl, ammonium nitrate, and ammonium sulfate) will take up water once the RH is high enough to exceed the solubility limit (deliquescence point) of the salt [Seinfeld and Panids, 2006].

3. Compare the mass of PM2.5 samples collected at the CDF site with those collected at the near-shoreline dune location, S1: In October 2019, samples were collected at both S1 and CDF. For days with high SLOAPCD BAM PM2.5, sea salt mass ranged from 0.1 to 1.8 $\mu g\ m^{-3}$ at CDF and from 0.3 to 2.8 $\mu g\ m^{-3}$ at S1. The nss dust mass ranged from 0.2 to 12.9 $\mu g\ m^{-3}$ at CDF and from 2.4 to 30.6 $\mu g\ m^{-3}$ at S1. The S1 site often had higher dust mass concentrations compared to samples collected simultaneously at CDF for two of three days, during which the S1 dust concentrations were more than 3 times higher than those at CDF. This result is consistent with the expectation that some PM2.5 particles that are lofted at S1 will be deposited back to the surface or mixed horizontally before reaching CDF, since particle concentration tends to decrease with increasing distance from the source.

4. Extend sampling of DNA from seawater, beach foam, and aerosol particles to test efficacy of Teflon air filters: The limited number of seawater and foam samples have provided valuable preliminary results, but further analysis is needed in order to interpret their implications. In particular, DNA extraction protocols for Teflon air filters used for particle mass measurements need to be evaluated. The seawater samples contained abundant dinoflagellate and diatom sequences but these were not found on the air filter. The air filters contained abundant common fungal spores from a non-marine source. The air filters contained abundant *Shewanella* bacterial sequences; *Shewanella* is typically a marine sediment bacterium. These sequences were found in one nearshore seawater sample and one of six dune samples so the results are ambiguous whether the cells on the filters are from the ocean or the dunes (indirectly from the oceans).

5. Characterize photosynthetic activity of phytoplankton offshore from the south San Luis County region: The photosynthetic activity of marine phytoplankton in the waters offshore and upwind of Oceano Dunes and adjacent south SLO County coastline is characterized by remotely-sensed estimates of chlorophyll and net primary production, NPP, in mg C $m^{-2}\ d^{-1}$). NPP is a combined measure of phytoplankton biomass and photosynthetic activity related to the phytoplankton biomass. NPP has been correlated with the production of sulfate aerosols as well as dimethyl sulfide (DMS), which is known to act as nuclei for aerosol formation (Charlson et al., 1987). Annual daily time series of NPP in the study area in 2019 show both very high productivity and high variability of phytoplankton associated with the dynamic effects of upwelling events as well as relaxations of upwelling activity. A series of daily distributions (images) of NPP in the study area (Figure 7) from the May 2019 sampling period (Figure 8) show the build-up of an area of high phytoplankton production area along the coast that is associated with an upwelling event. Time series of the daily mean NPP over the study area for the full year of 2019 is shown in Figure 9. The numerical values of mean NPP during the two field sampling periods are shown in Table 1.

Conclusions

PM2.5 mass concentrations at CDF show large but variable contributions of sea spray and mineral dust during high wind episodes when high BAM PM2.5 concentrations were also

recorded. For those sample collection days in May 2019, when the BAM PM2.5 exceeded 20 µg m^{-3}, sea salt varied from 1.1 to 1.8 µg m^{-3}, corresponding to 4% to 7% of BAM PM2.5, and nss dust from 4.1 to 14.4 µg m-3, corresponding to 26% to 46% of BAM PM2.5. The combined amounts of natural sea spray and inert mineral dust as determined by this investigation account for only 30% to 50% of the corresponding BAM PM2.5 concentration.

Organic components contributed only 1.1 to 1.8 µg m^{-3}, which was less than 6% of BAM PM2.5 on days when the BAM PM2.5 exceeded 20 µg m^{-3}. These results provide an upper limit on contributions from organic contributions from combustion, showing that the majority of chemically identified PM2.5 is not associated with fossil-fuel combustion or other emissions that are known to be toxic. This small contribution of fossil fuel combustion emissions to PM2.5 at the CDF location indicates that PM2.5 is not a good predictor of toxic emissions or health effects during high, west-northwesterly wind conditions. At the CDF location, a direct measure of toxics, as opposed to sea spray and mineral dust, is necessary in order to associate PM2.5 with health effects.

As determined from PM10 and PM2.5 measurements by SLOAPCD BAMs at the CDF location, as well as PM2.5 measurements by instruments deployed for this investigation, the association of high PM10 and PM2.5 with high wind conditions, rather than with weekends and holidays when OHV activity within the Oceano Dunes state park is high, indicates that dune dust is more likely generated by natural processes rather than vehicle activity. While the short duration of this study provides only limited statistics in support of this result, the more extensive PM records from the SLOAPCD CDF monitor provide ample confirmation. For this reason, the high dust concentrations measured on high wind days in and downwind of Oceano Dunes are likely dominated by natural saltation processes associated with the indigenous geomorphological dune structure.

There is a significant discrepancy in PM2.5 mass when comparing mass as measured by the SLOAPCD CDF PM2.5 BAM with the chemical mass of PM2.5 samples collected at the CDF location for this investigation. The PM2.5 from SLOAPCD BAM measurements is 42% to 63% greater than the sum of dust, salt, organic, and sulfate components. The PM2.5 mass difference is likely the result of contributions of mass from water, ammonium, nitrate, or other chemical species to measurements made by the SLOAPCD BAM instrument, though the difference may also be related to instrument calibration and operation. For this reason, offline chemical and gravimetric analyses would be needed in order to determine whether the SLOAPCD CDF BAM data are representative of actual PM2.5 concentrations at the CDF location and to determine what fraction of PM2.5 is dust.

Methods

Aerosol particle sampling used sharp-cut cyclones operated with calibrated flows to collect particles for analysis at ambient diameters below 1 µm and 2.5 µm (SCC 2.229 operated at 16.7 lpm and 7.5 lpm, respectively, BGI Inc., Waltham, MA). Teflon filters were used as substrates and showed negligible adsorption of volatile organic compounds (VOCs) on duplicate back filters collected simultaneously with each sample [Maria et al., 2003; Gilardoni et al., 2007]. The back filters provide a measure of adsorption during sampling and

contamination during handling (loading and unloading) and storage. Organic components collected on each back filter were analyzed as a measure of sampling error. Simultaneous samples were used to check for sampling consistency by comparing summed short to long samples, and long samples were used to check for groups present at low concentrations that fell below detection limit in the shorter samples.

Each sample (and associated back filter) was non-destructively analyzed by transmission FTIR. FTIR measurements of absorbance characterized the functional groups associated with major carbon bond types, including saturated aliphatic (alkane) groups, alcohol (used here to include phenol and polyol) groups, carboxylic acid groups, non-acidic carbonyl groups, and primary amine groups. The spectra were interpreted using an automated algorithm to perform baselining, peak-fitting, and integration with a revised version of the approach described previously [Maria et al., 2002; 2003; 2004; Maria and Russell, 2005; Russell et al., 2009; Takahama et al., 2013], using calibrations revised for the Tensor 27 spectrometer with RT-DLATGS detector (Bruker Optics, Ettlingen, Germany) [Gilardoni et al., 2007]. Additional calibrations of amines and carboxylic acids were used to improve accuracy by quantifying additional peaks at 2625 cm^{-1} and 2600-2800 cm^{-1}. Complete sets of internal standards for organic components of the atmosphere are not available, in part because the ambient particle composition is not fully known. In addition, the complexity of ambient mixtures of organic compounds in the atmosphere results in mixtures that cannot be fully resolved by FTIR. All of the measured functional groups are summed to calculate organic mass (OM). Estimates of the accuracy, errors, and detection limits of this technique for ambient measurements are discussed in Russell [2003].

X-ray Fluorescence (XRF) measurements were conducted by Chester LabNet (Tigard, OR) on the same filters used for FTIR to provide trace metal concentrations for elements heavier than Na [Maria et al., 2003]. Elemental concentrations were above detection for 30% to 100% of the ambient samples collected.

Surface chlorophyll-a concentration (Chla, mg m^{-3}) was estimated using standard NASA and ESA algorithms (O'Reilly et al., 1998; Hu et al., 2012) applied to MODIS-Aqua, MODIS-Terra, VIIRS-SNPP, VIIRS-JSPP1 (retrieved from NASA, https://oceancolor.gsfc.nasa.gov) and OLCI-A and OLCI-B (retrieved from EUMETSAT, https://oda.eumetsat.int) websites. Chlorophyll-a maps from individual sensors were merged at 1 km spatial resolution (https://www.wimsoft.com/CAL). Missing data due to clouds were minimized with a 5-day running mean filter. Daily net primary production (NPP, mg C m^{-2} day^{-1}) was calculated from daily datasets of Chla, photosynthetically active radiation (PAR, einstein m^{-2} day^{-1}) and sea-surface temperature (SST, C°) using the well-known VGPM algorithm (Behrenfeld and Falkowski, 1997) as empirically modified in Kahru et al. (2009, 2019). Daily datasets of PAR (Frouin et al., 1989) from individual sensors (MODIS-Terra, MODIS-Aqua, VIIRS-SNPP and VIIRS-JSPP1) were downloaded from https://oceancolor.gsfc.nasa.gov and merged. Daily SST datasets were downloaded as optimally interpolated sea-surface temperature (OISST) (Reynolds et al., 2007) from https://www.ncdc.noaa.gov/oisst. A study area of 120 km (east-west) x 100 km (north-south) west of Pismo Beach was used to create time series (Fig. 7). Daily means of all valid pixels for the study area are reported here but full statistics are available.

Acknowledgments

References

Apte, J. S., M. Brauer, A. J. Cohen, M. Ezzati, and C. A. Pope (2018), Ambient PM2.5 Reduces Global and Regional Life Expectancy, Environmental Science & Technology Letters, 5(9), 546-551, doi:10.1021/acs.estlett.8b00360.

Behrenfeld, M.J., Falkowski, P.G., 1997. Photosynthetic rates derived from satellite based chlorophyll concentration. Limnol. Oceanogr. 42, 1-20.

Chen, C. L., et al. (2018), Organic Aerosol Particle Chemical Properties Associated with Residential Burning and Fog in Wintertime San Joaquin Valley (Fresno) and With Vehicle and Firework Emissions in Summertime South Coast Air Basin (Fontana), Journal of Geophysical Research-Atmospheres, 123(18), 10707-10731, doi:10.1029/2018jd028374.

Dockery, D. W. (1993), Epidemiologic-Study Design for Investigating Respiratory Health-Effects of Complex Air-Pollution Mixtures, Environmental Health Perspectives, 101, 187-191, doi:10.2307/3431676.

Frouin, R., Ligner, D.W., Gautier, C., 1989. A simple analytical formula to compute clear sky total and photosynthetically available solar irradiance at the ocean surface. J. Geophys. Res. 94, 9731-9742.

Gilardoni, S., et al. (2007), Regional variation of organic functional groups in aerosol particles on four US east coast platforms during the International Consortium for Atmospheric Research on Transport and Transformation 2004 campaign, Journal of Geophysical Research-Atmospheres, 112(D10), doi:10.1029/2006jd007737.

Gwinn, M. R., and V. Vallyathan (2006), Nanoparticles: Health effects - Pros and cons, Environmental Health Perspectives, 114(12), 1818-1825, doi:10.1289/ehp.8871.

Hoek, G., B. Brunekreef, S. Goldbohm, P. Fischer, and P. A. van den Brandt (2002), Association between mortality and indicators of traffic-related air pollution in the Netherlands: a cohort study, Lancet, 360(9341), 1203-1209, doi:10.1016/s0140-6736(02)11280-3.

Hu, C., Z. Lee, and B. Franz (2012), Chlorophyll a algorithms for oligotrophic oceans: A novel approach based on three-band reflectance difference, J. Geophys. Res., 117, C01011, doi:10.1029/2011JC007395.

Janssen, N. A. H., B. Brunekreef, P. van Vliet, F. Aarts, K. Meliefste, H. Harssema, and P. Fischer (2003), The relationship between air pollution from heavy traffic and allergic sensitization, bronchial hyperresponsiveness, and respiratory symptoms in Dutch schoolchildren, Environmental Health Perspectives, 111(12), 1512-1518, doi:10.1289/ehp.6243.

Jimenez, J. L., et al. (2009), Evolution of Organic Aerosols in the Atmosphere, Science, 326(5959), 1525-1529.

Kahru, M., Kudela, R., Manzano-Sarabia, M., Mitchell, B.G., 2009. Trends in primary production in the California Current detected with satellite data. J. Geophys. Res. Ocean. 114, 1–7 https://doi.org/10.1029/2008JC004979.

Kahru, M., R. Goericke, T.B. Kelly, M.R. Stukel (2019), Satellite estimation of carbon export by sinking particles in the California Current calibrated with sediment trap data, Deep-Sea Research, Part II, 104639, ISSN 0967-0645, https://doi.org/10.1016/j.dsr2.2019.104639.

Knol, A. B., et al. (2009), Expert elicitation on ultrafine particles: likelihood of health effects and causal pathways, Particle and Fibre Toxicology, 6, doi:10.1186/1743-8977-6-19.

Maria, S. F., and L. M. Russell (2005), Organic and inorganic aerosol below-cloud scavenging by suburban New Jersey precipitation, Environmental Science & Technology, 39(13), 4793-4800, doi:10.1021/es0491679.

Maria, S. F., L. M. Russell, M. K. Gilles, and S. C. B. Myneni (2004), Organic aerosol growth mechanisms and their climate-forcing implications, Science, 306(5703), 1921-1924, doi:10.1126/science.1103491.

Maria, S. F., L. M. Russell, B. J. Turpin, and R. J. Porcja (2002), FTIR measurements of functional groups and organic mass in aerosol samples over the Caribbean, Atmospheric Environment, 36(33), 5185-5196, doi:10.1016/s1352-2310(02)00654-4.

Maria, S. F., L. M. Russell, B. J. Turpin, R. J. Porcja, T. L. Campos, R. J. Weber, and B. J. Huebert (2003), Source signatures of carbon monoxide and organic functional groups in Asian Pacific Regional Aerosol Characterization Experiment (ACE-Asia) submicron aerosol types, Journal of Geophysical Research-Atmospheres, 108(D23), doi:10.1029/2003jd003703.

McDonald, B. C., et al. (2018), Volatile chemical products emerging as largest petrochemical source of urban organic emissions, Science, 359(6377), 760-764, doi:10.1126/science.aaq0524.

NARSTO (2004), Particulate Matter Science for Policy Makers: A NARSTO Assessment, Cambridge, England.

O'Reilly, J.E., S. Maritorena, B.G. Mitchell, D. A. Siegel, K. L. Carder, S. A. Garver, M. Kahru, and C. R. McClain (1998), Ocean color chlorophyll algorithms for SeaWiFS, J. Geophys. Res., 103, 24937–24953.

Oberdorster, G., V. Stone, and K. Donaldson (2007), Toxicology of nanoparticles: A historical perspective, Nanotoxicology, 1(1), 2-25, doi:10.1080/17435390701314761.

Palenik, B., Nagarkar, M., (2018), Marine contributions to aerosol particulates in a coastal environment. Report prepared for the California Department of Parks and Recreation and the California Geological Survey, March 6, 2018.

Pope, C. A., M. Ezzati, and D. W. Dockery (2009), Fine-Particulate Air Pollution and Life Expectancy in the United States, New England Journal of Medicine, 360(4), 376-386, doi:10.1056/NEJMsa0805646.

Reynolds, R.W., Smith, T.M., Liu, C., Chelton, D.B., Casey, K.S., Schlax, G., 2007. Daily high-resolution blended analyses for sea surface temperature. J. Clim. 20, 5473-5496, https://doi.org/10.1175/2007JCLI1824.1

Russell, L. M. (2003), Aerosol organic-mass-to-organic-carbon ratio measurements, Environmental Science & Technology, 37(13), 2982-2987, doi:10.1021/es026123w.

Russell, L. M., R. Bahadur, and P. J. Ziemann (2011), Identifying organic aerosol sources by comparing functional group composition in chamber and atmospheric particles, Proceedings of the National Academy of Sciences of the United States of America, 108(9), 3516-3521, doi:10.1073/pnas.1006461108.

Russell, L. M., L. N. Hawkins, A. A. Frossard, P. K. Quinn, and T. S. Bates (2010), Carbohydrate-like composition of submicron atmospheric particles and their production from ocean bubble bursting, Proceedings of the National Academy of Sciences of the United States of America, 107(15), 6652-6657, doi:10.1073/pnas.0908905107.

Russell, L. M., S. Takahama, S. Liu, L. N. Hawkins, D. S. Covert, P. K. Quinn, and T. S. Bates (2009), Oxygenated fraction and mass of organic aerosol from direct emission and atmospheric processing measured on the R/V Ronald Brown during TEXAQS/GoMACCS 2006, Journal of Geophysical Research-Atmospheres, 114, doi:10.1029/2008jd011275.

Seinfeld, J. H., and S. N. Pandis (2006), Atmospheric Chemistry and Physics: From Air Pollution to Climate Change, Second ed., John Wiley & Sons, Hoboken, New Jersey.

Takahama, S., A. Johnson, and L. M. Russell (2013), Quantification of Carboxylic and Carbonyl Functional Groups in Organic Aerosol Infrared Absorbance Spectra, Aerosol Science and Technology, 47(3), 310-325, doi:10.1080/02786826.2012.752065.

Takahama, S., R. E. Schwartz, L. M. Russell, A. M. Macdonald, S. Sharma, and W. R. Leaitch (2011), Organic functional groups in aerosol particles from burning and non-burning forest emissions at a high-elevation mountain site, Atmospheric Chemistry and Physics, 11(13), 6367-6386, doi:10.5194/acp-11-6367-2011.

Usher, C. R., A. E. Michel, and V. H. Grassian (2003), Reactions on Mineral Dust, Chemical Reviews, 103(12), 4883-4940, doi:10.1021/cr020657y.

Zhang, Q., et al. (2007), Ubiquity and dominance of oxygenated species in organic aerosols in anthropogenically-influenced Northern Hemisphere midlatitudes, Geophysical Research Letters, 34(13), 6, doi:10.1029/2007gl029979.

Table

Table 1. Mean NPP (mg C m^{-2} d^{-1}) for the study area during the two sampling periods.

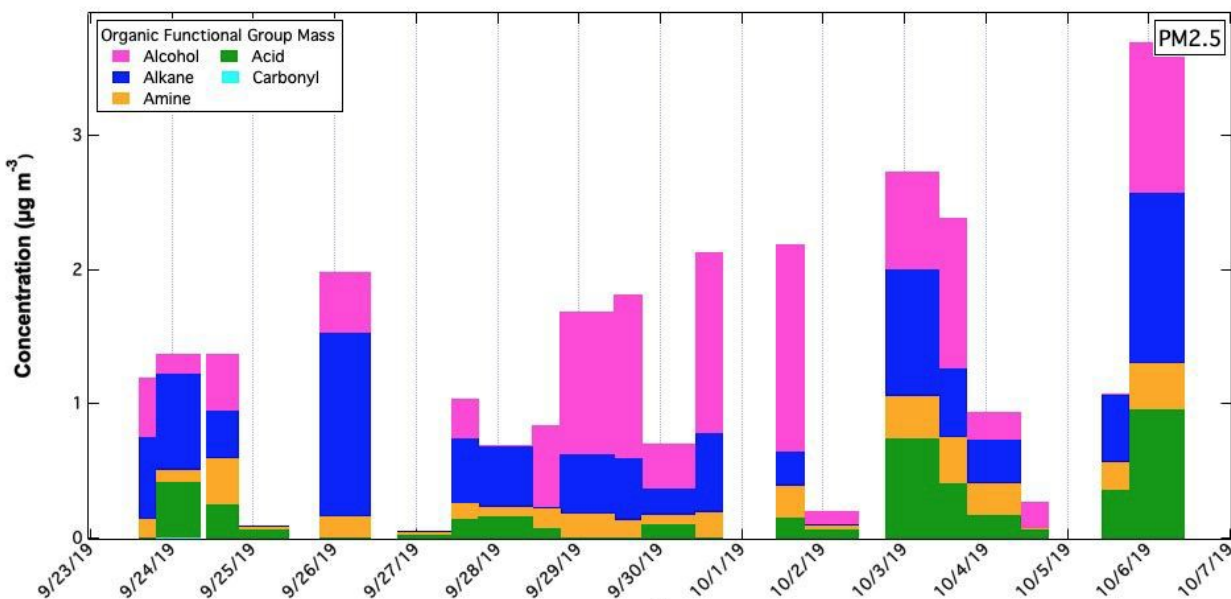| Date	Day of year	Mean NPP		Date	Day of year	Mean NPP
5/15/201	135	833.6		9/23/2019	266	4353
5/16/201	136	885.9		9/24/2019	267	3828
5/17/201	137	915.6		9/25/2019	268	3806
5/18/201	138	810.7		9/26/2019	269	3516
5/19/201	139	1004.1		9/27/2019	270	3335
5/20/201	140	933.9		9/28/2019	271	3668
5/21/201	141	943.5		9/29/2019	272	3837
5/22/201	142	1024.0		9/30/2019	273	3734
5/23/201	143	991.9		10/1/2019	274	3507
5/24/201	144	1115.1		10/2/2019	275	3517
5/25/201	145	1962.6		10/3/2019	276	3360
5/26/201	146	1800.6		10/4/2019	277	3510
5/27/201	147	2112.1		10/5/2019	278	3407
5/28/201	148	1966.1		10/6/2019	279	3668
5/29/201	149	1984.6		10/7/2019	280	4033
5/30/201	150	2904.9				
5/31/201	151	669.9				
6/1/201	152	748.4				
6/2/201	153	345.7				

Figures
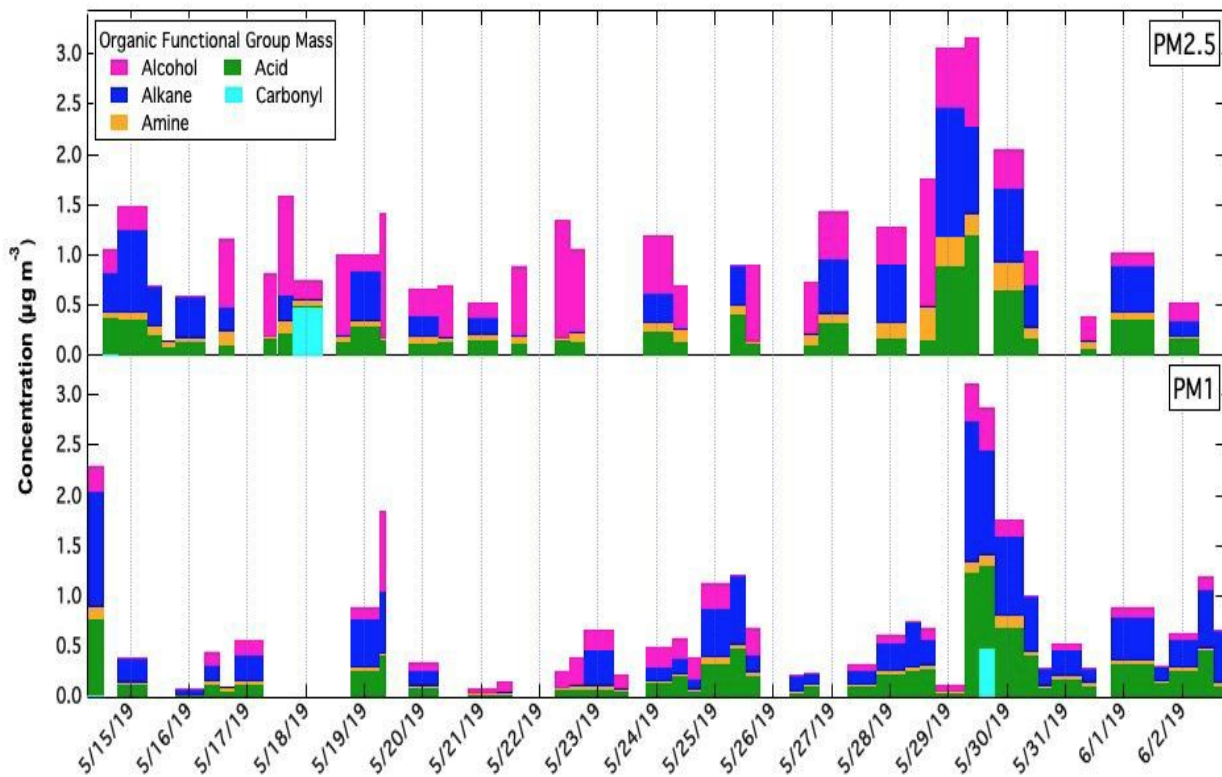
Figure 1. May 2019 PM2.5 and PM1 organic functional group (OFG) mass concentration [µg m^{-3}] measurements by FTIR at CDF. Samples below detection are not shown. Note that a high alkane OFG mass is likely representative of fossil fuel combustion emissions from man-made sources, and that a high ratio of alcohol OFG mass to alkane OFG mass is indicative of marine sea spray organic sources (e.g., phytoplankton). The FTIR measurements show qualitatively that there were different sources of organic mass present since the mixture of OFG varies from day to day. The two types of mixtures evident in the FTIR analyses of the samples collected: One shows a high ratio of alcohol OFG mass to alkane OFG mass, indicating sea spray. The other mixture is mostly alkane OFG mass with amine OFG mass, which may indicate either fossil fuel combustion (including vehicles) or sea spray. Some samples are a mixture of both of these two types. There are also carboxylic acid groups present in a majority of samples, which typically indicate oxidation of volatile organic carbon emissions by photochemistry.
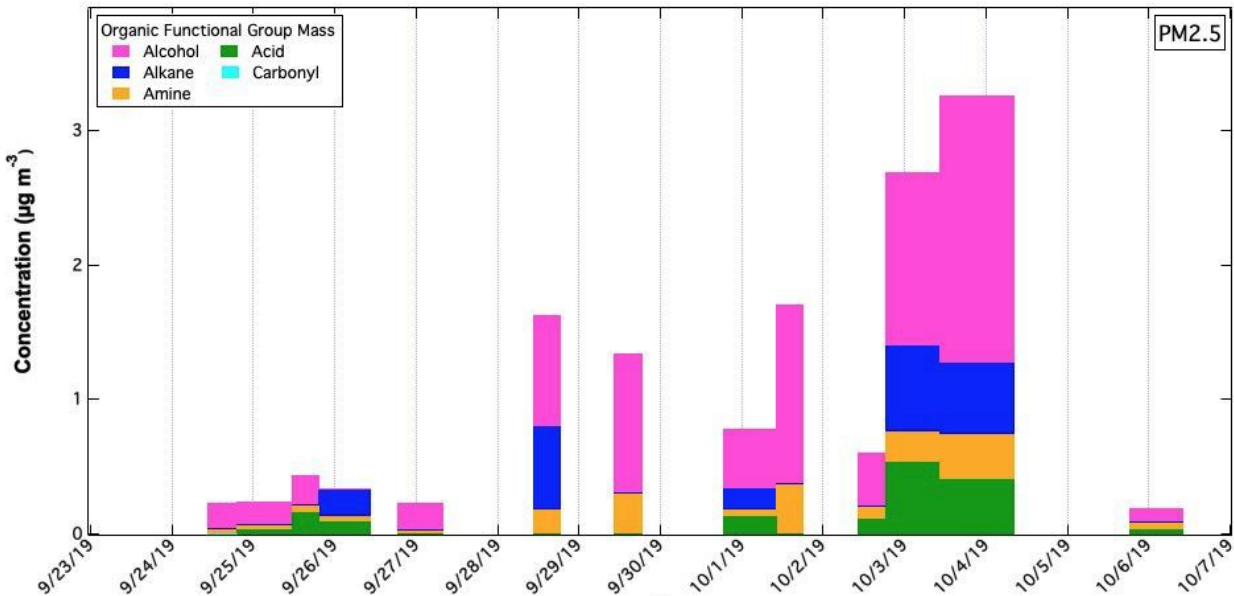
Figure 2. October 2019 PM2.5 organic functional group mass concentration [μg m-3] measurements by FTIR at CDF. Samples below detection are not shown. Note that a high alkane OFG mass is likely representative of fossil fuel combustion emissions from man-made sources, and that a high ratio of alcohol OFG mass to alkane OFG mass is indicative of marine sea spray organic sources (e.g., phytoplankton). The FTIR measurements show qualitatively that there were different sources of organic mass present since the mixture of OFG varies from day to day. The two more frequent types of mixtures evident in the FTIR analyses of the samples collected: One shows a high ratio of alcohol OFG mass to alkane OFG mass, indicating sea spray. The other mixture is mostly alkane OFG mass with amine OFG mass, which may indicate either fossil fuel combustion (including vehicles) or sea spray. Some samples are a mixture of both of these two types. There are also carboxylic acid groups present in a majority of samples, which typically indicate oxidation of volatile organic carbon emissions by photochemistry.
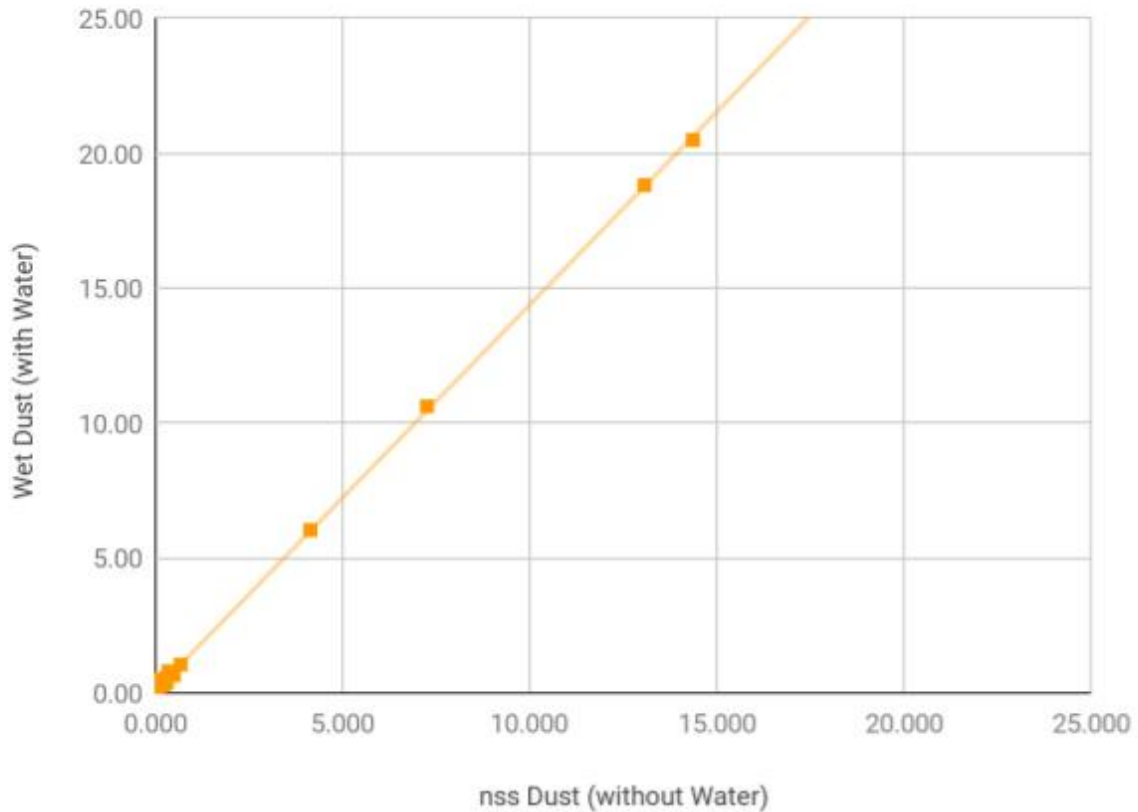
Figure 3. October 2019 PM2.5 organic functional group mass concentration [μg m-3] measurements by FTIR at S1 in the Oceano Dunes. Samples below detection are not shown. Note that a high alkane OFG mass is likely representative of fossil fuel combustion emissions from man-made sources, and that a high ratio of alcohol OFG mass to alkane OFG mass is indicative of marine sea spray organic sources (e.g., phytoplankton). The FTIR measurements show qualitatively that there were different sources of organic mass present since the mixture of OFG varies from day to day. The two more frequent types of mixtures evident in the FTIR analyses of the samples collected: One shows a high ratio of alcohol OFG mass to alkane OFG mass, indicating sea spray. The other mixture is mostly alkane OFG mass with amine OFG mass, which may indicate either fossil fuel combustion (including vehicles) or sea spray. Some samples are a mixture of both of these two types. There are also carboxylic acid groups present in a majority of samples, which typically indicate oxidation of volatile organic carbon emissions by photochemistry.

Figure 4. Comparison of estimated dust mass concentration mass concentration [μg m^{-3}] measurements for nss dust and wet dust for May 2019 samples with XRF measurements. The nss dust consists of minerals and excludes sea salt [Usher et al., 2003]. Wet dust was quantified from PM2.5 mass that was resuspended from surface sand that was collected on 28 September 2019. These two approaches provide estimates for the mineral component mass (nss dust) and for the higher mass that could be associated with dust at ambient relative humidity (wet dust). The comparison of the two approaches indicates that the "wet dust" approach accounted for approximately 50% additional mass from water. This means that the two methods are consistent in terms of the amount of mass associated with specific measured elements. It also provides preliminary evidence that water could be a substantial fraction (50%) of both surface sand and lofted dust.
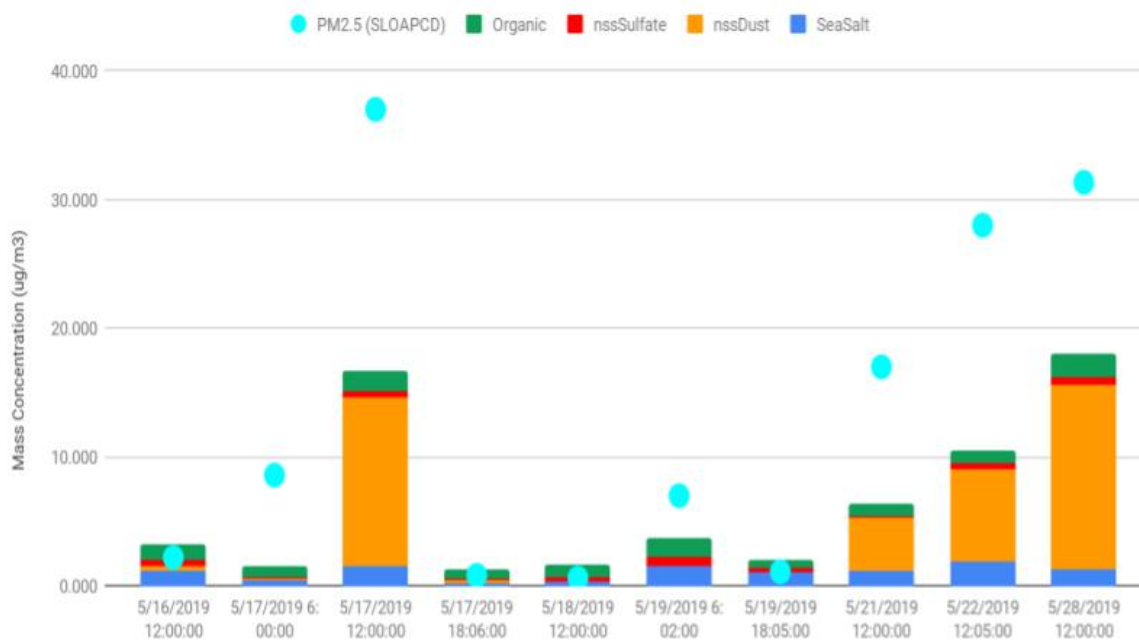
Figure 5. May 2019 PM2.5 mass concentration [μg m-3] from SLOAPCD BAM measurements and chemical mass concentrations [μg m-3] from FTIR and XRF measurements at CDF. Labels provide filter start times and dates, with duration of approximately 6 hr for daytime and 12 hr for nighttime. SLOAPCD BAM values are calculated as the average of hourly concentrations for the duration of the corresponding filter samples. Samples below detection are not shown. The graph shows that for May samples for which SLOAPCD BAM measurements of PM2.5 exceeded 20 μg m-3 and all chemical components were above detection (May 17, 22, and 28), the salt, nss dust, organic, and sulfate accounted for 38% to 57% of the averaged hourly BAM PM2.5 measurements, indicating a PM2.5 mass discrepancy between samples collected for this investigation and temporally corresponding PM2.5 mass measurements made by the SLOAPCD CDF BAM. For days in May 2019 with BAM 2.5 exceeding 20 μg m-3, sea salt varied from 1.1 to 1.8 μg m-3, corresponding to 4% to 7% of BAM PM2.5, and nss dust from 4.1 to 14.4 μg m-3, corresponding to 26% to 46% of BAM PM2.5. Organic components contributed only 1.1 to 1.8 μg m-3, which was less than 6% of BAM PM2.5 on days with BAM PM2.5 exceeding 20 μg m-3.

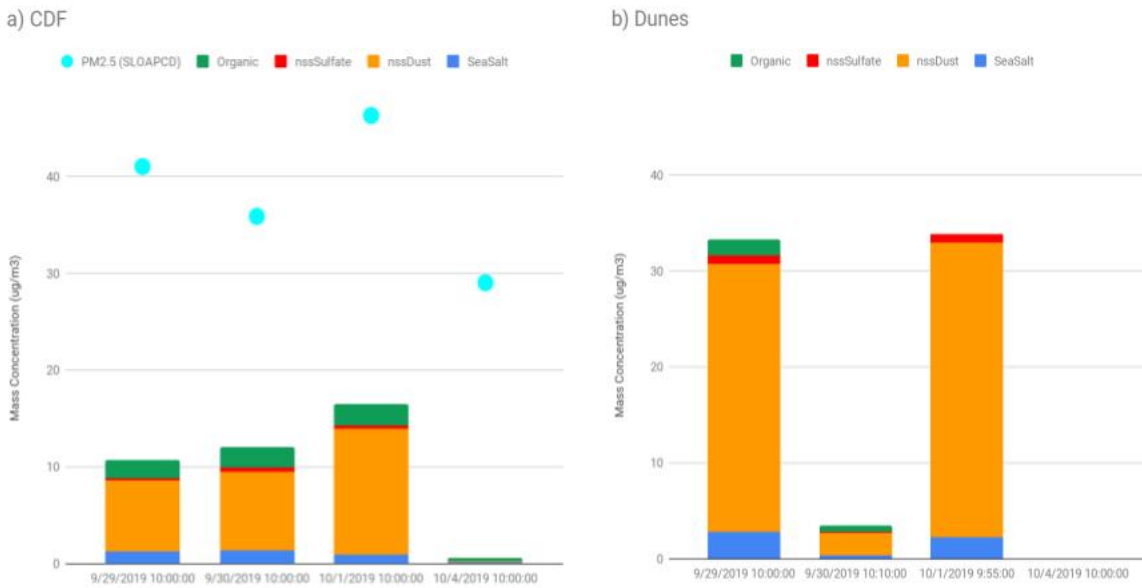Figure 6. Sept-Oct 2019 PM2.5 mass concentration [μg m-3] from SLOAPCD BAM measurements and chemical mass concentrations [μg m-3] from FTIR and XRF measurements at (a) CDF and (b) Dunes (S1). Labels provide filter start times and dates, with duration of approximately eight hours. SLOAPCD BAM values are calculated as the average of hourly concentrations for the duration of the corresponding filter samples. Components below detection are not shown; sample for 4 October 2019 at Dunes was not available. For days with high SLOAPCD BAM PM2.5, sea salt mass ranged from 0.1 to 1.8 μg m^{-3} at CDF and from 0.3 to 2.8 μg m^{-3} at S1. The nss dust mass ranged from 0.2 to 12.9 μg m^{-3} at CDF and from 2.4 to 30.6 μg m^{-3} at S1. The S1 site often had higher dust mass concentrations compared to samples collected simultaneously at CDF for two of three days, during which time the S1 dust concentrations were more than 3 times higher than those at CDF.

Figure 7. Study area (black) used to construct NPP time series west of Pismo Beach, California and vicinity.
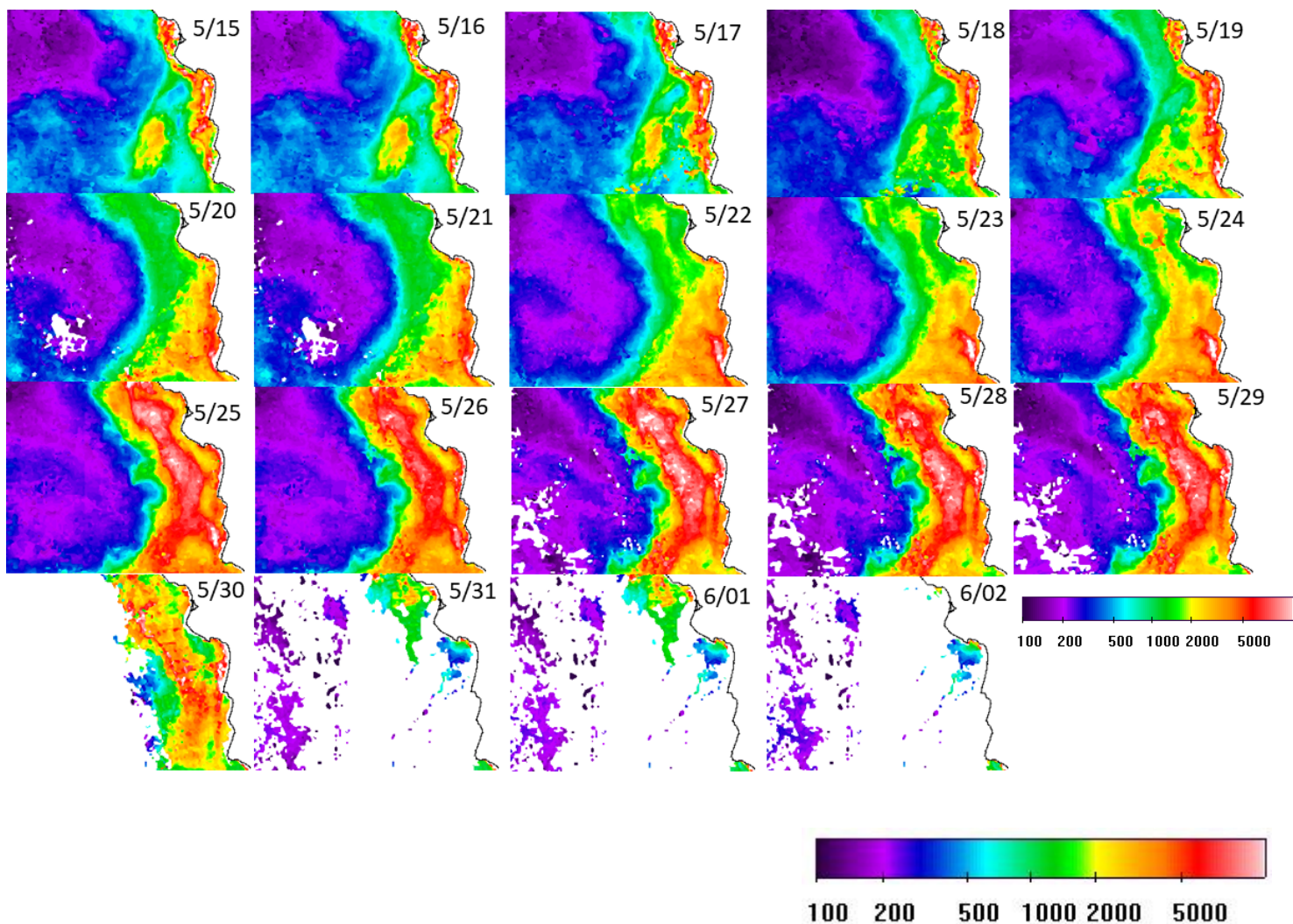
Figure 8. Series of daily NPP (mg C m^{-2} d^{-1}) images in the study area from 5/15/2019 through 6/2/2019. Cloudy conditions indicated by lack of data for days 5/30/2019 through 6/2/2019.
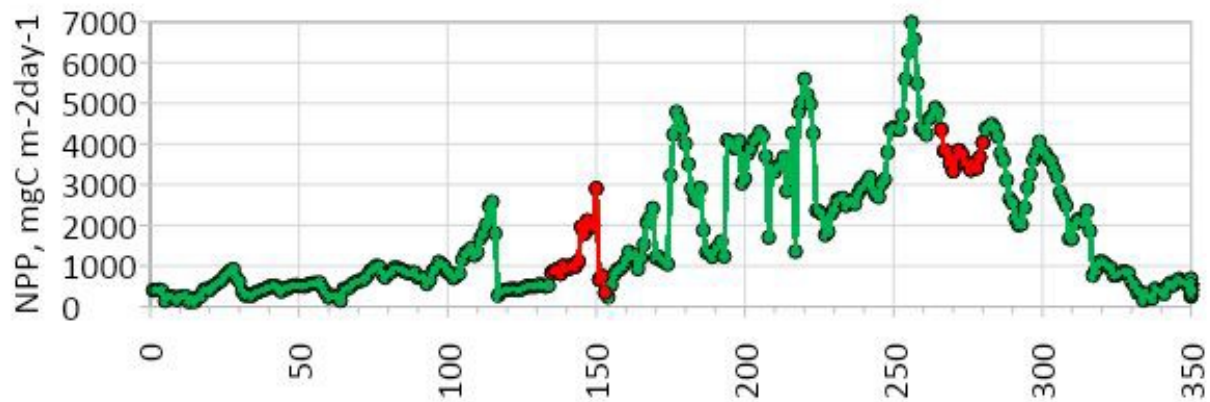
Figure 9. Time series of the mean NPP over the study area for the full year of 2019 (versus day of the year). The NPP sampling periods of 5/15/2019 to 6/2/2019 (days 135-153) and 9/23/2019 to 10/7/2019 (days 266-280) are shown in red.